Inhibiting Property of Phytoconstituents of 'Aconitum Heterophyllum' Against Omicron Variant of SARS-CoV-2: Molecular Docking, Molecular Dynamic and MM-GBSA approach

Shradha Lakhera
   Uttarakhand Open University

Kamal Devlal
   Uttarakhand Open University

Meenakshi Rana (✉ mrana@uou.ac.in)
   Uttarakhand Open University

Arabinda Ghosh
   Guwahati University: Gauhati University

Abstract

Omicron's traces have been found significantly faster than the Delta variant. Persons who already have been vaccinated are also affected by this variant. This shows that vaccines taken to combat COVID-19 are less effective in preventing the Omicron's transmission. Thus, the identification of effective candidates to fight against Omicron has been the top priority in pharmaceutics. The present study deals with the investigation of the antiviral activities of the phytocompounds of Aconitum heterophyllum against the Omicron variant. The systematic *in-silico* study done in the paper reveals the good binding of Isoatisine with spike glycoprotein of Omicron. Isoatisine molecule follows most of the pharmacokinetic properties that make it a better drug-like molecule. The computed global reactivity parameters fairly justified the high reactivity of the Isoatisine molecule. This study aims to discover the novel antiviral activity of Isoatisine to counter the Omicron protein. The results of this study can also be considered for experimental validation and clinical trials.

1. Introduction

SARS-CoV-2 is a very well-known and ongoing disaster in humankind. It had devastating effects on people worldwide and for the last three years, humankind had to suffer a consistent fear of death. The day-by-day mutating variants of the virus are increasing the problems of medicinal scientists and researchers. It is the very first known and the globally distributed variant was the Alpha (B.1.1.7 linage) variant [1]. After that, various variants emerged like beta, gamma delta, mu, and many more [2]. These variants mutated and their genome leads to the modulation of the virus. The results of the mutations of these variants are in our sights. Various vaccines were also introduced and a large part of the global population was given vaccines. But the virus is still developing its variants. Recently, in November 2021, Omicron infected cases arrived in South Africa and the World health organization (WHO) declared Omicron as a new variant of COVID-19 [3]. This variant has shown numerous spike-mutations as compared to the other previously known variants [4]. Thus, this variant was named the variant of concern (VOC) by WHO [5]. In a very less time of about two months, this variant has infected at least 108 countries and more than 15 lakh cases have been reported worldwide [6]. Structural changes in the spike-glycoprotein are observed in the Omicron which leads to a large number of mutations in the angiotensin-converting enzyme2 (ACE2) binding sites [7]. Major known mutations of Omicron are SARS-CoV-2501.V2 (B.1.351 lineage), variant B.1.1.529, and VOC 202012/01 (B.1.1.7 lineage) [8]. These variants hold on to mutations of spike protein receptor-binding domain (RBD) that result in the binding of virus proteins to human ACE2 [9]. The study so far claimed the higher binding of Omicron spike-glycoproteins with the ACE2 results in a rise in infection and transmission [10]. However, the high fatality rate of this variant is not recorded so far, but the sustained mutation of this variant may lead to tragic conditions. Thus, drug development is highly needed to terminate this mutation.

On the other hand, herbal extracts had been the frontline warriors throughout the pandemic. People were seen to depend on the herbal aids to revolt against COVID-19. Many homemade remedies for improving the immunity of the body. The literature survey accounts for numerous simulation studies that targeted

various variants of COVID-19. Various herbal extracts like I-Asarinin [11], Parthenolide [12], Berberine [13], beta-sitosterol [14], choline [15], etc have been used for inhibiting the proteins of COVID-19. The Himalayan region is known as the heart of medicinal herbs. Thousands of the varieties of medicinal plants are found in the Himalayan region that holds many medicinal benefits and is known to cure many diseases since Vedic times. One such herbal plant namely, Aconitum Heterophyllum is targeted for this study. This plant is a native of Himalayan foothills, and apart from Uttarakhand, it is also found in Nepal [16]. Regionally, it is named "atish" or "ativisha" and it is a flowering plant [17]. It is found at altitudes between 2,500 m to 4,000 m [18]. This plant has lots of health benefits like they are used as an expectorant, febrifuge, anthelmintic, anti-diarrhoeal, anti-emetic, and anti-inflammatory [19]. The toxicity of the extracts of this plant makes it usable as an anti-poison agent against scorpion or snake bites [20]. Many studies report the use of Aconitum heterophyllum extracts for the treatment of breast cancer [21], artiritis [22], Alzheimer's [23], diarrhea [24], and many more. It is also used to cure fever and contagious diseases which is the main reason to target it as an inhibitor against the COVID-19 variant. As the primary symptom of the Omicron is fever, this is believed that this plant can inhibit the virus and work against its symptoms. This study leads to the identification of a novel phytocompound of Aconitum heterophyllum that can show the inhibitory potentiality against the COVID-19 Omicron variant. The morphology of the plant is illustrated in Fig. 1.

Aconitum heterophyllum has a wide variety of phytochemicals like 14-Anisoylaconine, 6-Acetylheteratisine, 6-Benzoylheteratisine, Aconitine, Atidine, Atisine, Benzoylmesaconine, Dihydroatisine, Heterophyllisine, heterophylloidine, Hetidine, Hetisine, Hetisinone, Isoatisine, Jesaconitine, Lappaconitine, Mesaconitine, Phytosterols, Aricine, beta-carotene, Delphatines, Hypaconitine, lactone atisenol, Lycoctonine, and Veratridie. Molecular docking was performed for all the fifteen phytochemicals and the best-docked ligands were selected. Pharmacokinetic properties of the best-docked ligands were also analyzed to check the proper drug-like behavior. The chemical reactivity of the selected ligand was computed using density functional theory (DFT). The structure optimization was done to fetch the reactivity parameters within the ligand. The Molecular Dynamics (MD) simulation was performed for the best protein-ligand complex to check the stability of the complex. The MD Simulation reveals the stability of the complex and also justifies whether the ligand can be a potential inhibitor or not.

2. Materials And Methods

2.1 Potential target protein receptor and Potential inhibitor preparation

The structure of the target protein for the present study was downloaded from the database "Protein Data Bank" (https://www.rcsb.org/). The protein of the omicron variant of SARS-CoV-2 with spike glycoprotein in complex with Beta-55 and EY6A (PDB ID: 7QNW) was considered as the target protein. This target protein is a 5-chain macromolecule having a resolution of 2.40 Å. This selection was done as this protein has a suitable resolution and is found in homo sapiens. The protein structure of the protein is illustrated

in Fig. 2. The structures of ligands were downloaded from the database "IMPPAT" (https://cb.imsc.res.in/imppat/home) and their 3-D structures are shown in SD. 1.

3. Computational Procedure And Calculation

The systematic *in-silico* study had been performed for the selected phytochemicals following the steps. Firstly, molecular docking was performed to check the binding of the ligands to the active sites of the protein. The docking is done using the software, "Autodock Vina" (https://vina.scripps.edu/). Further, the screening of drug-like properties of the phytochemicals having the best binding affinity. The path followed by the drug inside the human body right after consumption and the metabolism of the drug inside the body is accounted for by the ADMET properties. The ADMET properties were analyzed using the database, "SwissADME" (http://www.swissadme.ch/). Furthermore, the ligand with most of the drug-like properties followed was selected as the most favorable ligand and a reactivity check was done with the selected ligand. The reactivity parameters were analyzed by performing structure optimization using "Gaussian09" [25] software. The DFT was used for the structure optimization with B3LYP/6311-G basis set [26, 27]. Different global reactivity parameters were computed for the selected ligand for investigating its reactivity. The calculation of global reactivity parameters was done using Koopman's equations which are the same as mentioned in the cited papers [28, 29]. The results of the optimization were analyzed by software, "Gauss View" [30]. The stability of the complex obtained by docking was investigated by performing the MD Simulation in the final step. The software, "Desmond modules vs 2020.1 (https://www.schrodinger.com/)" was used for performing MD Simulation [31]. The OPLS2005 force field was used for the availability of larger coverage of organic functionality. For the neutralization of charge, 11 Na+, and 8 Cl- counter ions are added. Simple Point Charge (SPC) is also used to fetch the correct density and permittivity. The Simulation continued till 50 ns at the conditions of the Isothermal-Isobaric ensemble (constant number of particles, Pressure, Temperature) (NPT). Simulation interaction diagrams are studied with the help of the Desmond GUI tool Maestro. Parameters obtained in a simulation like Root-Mean Square Deviation (RMSD), Root Mean Square Fluctuation (RMSF), number of H-bonds, and Radius of Gyration were used to justify the stability of the complex. The trajectories of the MD parameters were plotted using software, "Originlab2021(https://www.originlab.com/)" [32]. During MD simulations of SARS-CoV-2 with spike glycoprotein complexed with ligand, the binding free energy (G_{bind}) of docked complexes was calculated using molecular mechanics generalized Born surface area (MM-GBSA) module [33]. The binding free energy was calculated using the OPLS 2005 force field, VSGB solvent model, and rotamer search methods. After the MD run, 10 ns intervals were used to choose the MD trajectories frames. The total free energy binding was calculated using Eq. 1:

$$\Delta G_{bind} = G_{complex} - (G_{protein} + G_{ligand}) \dots\dots\dots\dots\dots\dots\dots\dots (1)$$

Where ΔG_{bind} = binding free energy, $G_{complex}$ = free energy of the complex, $G_{protein}$ = free energy of the target protein, and G_{ligand} = free energy of the ligand. The MMGBSA outcome trajectories were analyzed further for post dynamics structure modifications.

4. Results And Discussions

4.1 Molecular Docking and ADMET Analysis

The molecular docking provides the binding strengths of the ligands with the target protein. The docking scores of the considered ligands are mentioned in SD. 2. Generally, the docking scores less than − 6 kcal/mol are considered as the good binding scores [34, 35]. In the recent study, all the considered phytochemicals have a binding affinity of less than − 6 kcal/mol. Selecting the ligands with the best binding affinity, 6-Benzoylheteratisine, Heterophylloidine, Hetisine, Isoatisine, and Veratridine have the binding affinity of -8.1, -8.0, -8.0, -8.1, and − 8.4 kcal/mol. Thus, these phytochemicals have good fitting inside the binding pocket of the protein.

The ADMET properties were analyzed for the prediction of the drug-like properties of the ligands. The pharmacokinetic properties of the ligands are mentioned in the SD. 3. 6-Benzoylheteratisine follows Lipinski, Veber, egan, and Mugge's rule but fails to follow ghose filters. It also does not have required blood-brain-barrier penetration which leads to the rejection of 6-Benzoylheteratisine as a drug-like molecule. Hetisine follows all the pharmacokinetic rules but fails to have BBB permeability. Heterophylloidine and Isoatisine are the phytochemicals following all of the rules. Thus, these molecules are more likely to behave as drug-like molecules. The docking scores for Heterophylloidine and Isoatisine are − 8.0, and − 8.1 kcal/mol respectively. Veratridine has the binding affinity of -8.4 kcal/mol but it fails to follow Lipinski, ghose, egan, mugge, and Veber rules. The GI absorption is also low for the Veratridine molecule. It doesn't have BBB penetration. Despite of having better binding affinity than other ligands, Veratridine doesn't behave as a drug-like molecule. Isoatisine molecule has the best binding affinity among all the other ligands. The ligand binds to the surface glycoprotein chain of the protein and the illustration of the residues associated with the binding is shown in Fig. 3. There are three conventional hydrogen bonds associated with this binding. The amino acid residues TYR55, ASN439, and GLN506 leads to these conventional hydrogen bonds. Residues ARG33 and LYS440 impart in the alkyl bond formation. The binding pose of ligand to protein has drieding energy of 118.64 kcal/mol and 2.062 Debye. The docking details of the conventional hydrogen bond and alkyl interactions are mentioned in SD. 4 and the protein-ligand illustration is shown in SD. 5 and SD. 6.

4.2 Reactivity analysis

The reactivity of the Isoatisine molecule was investigated by using an optimized structure. The geometry of Isoatisine was non-planar having one pyrrolidine ring and one hydroxyl group associated with it. The atoms 2O − 56H make the hydroxyl group. Mulliken charge distribution shows the charge variation between the atoms of the pyrrolidine and the hydroxyl groups. Charge associated to the atoms of pyrrolidine ring are 15C (0.334e), 3N (-0.564e), 23C (-0.225e), 24C (-0.059e), and 1O (-0.511e) whereas the 2O and 56H atoms of hydroxyl groups have charge − 0.579e and 0.354e respectively. Thus, intramolecular charge transfer (ICT) was observed by the charge distribution. The existence of the ICT was verified by the molecule's MEP surface illustrated in Fig. 4. The nucleophilic region was shaded near

the pyrrolidine ring and the electrophilic region is settled near the hydroxyl group. This validates the occurrence of ICT from the pyrrolidine ring towards the hydroxyl group.

The frontier molecular orbitals (FMO), sometimes called global reactivity parameters were computed to detect the chemical reactivity of the Isoatisine molecule. The molecule must be chemically reactive to be a drug-like molecule. The energies corresponding to HOMO and LUMO (Highest occupied and lowest unoccupied molecular orbitals) were used for computing the parameters. The HOMO-LUMO are known as FMO as they are the primary molecular orbitals to show the electronic transitions. The energy gap between these orbitals shows whether the electrons in the molecule are capable enough to transit to the higher energy states. The energy gap between HOMO-LUMO for Isoatisine was computed as 5.435 eV. The moderate value of the energy gap shows the possibility of electronic excitations. This value can also be incorporated as the stability of the probe molecule. The dislocation of the HOMO-LUMO surface justifies the electron excitation (Fig. 5(a)). The HOMO-LUMO surfaces are represented as the red and green color surfaces. These surfaces show positive and negative phases in molecular orbital wave function. These surfaces are settled over the pyrrolidine ring in the HOMO while in the case of LUMO, these surfaces are distributed over the hydroxyl group. This variation shows the displacement of the charge cloud from the pyrrolidine ring to the hydroxyl group. Thus, the displacement of the orbital surfaces leads to the ICT. The values of FMO parameters are also favorable (SD. 7). The high value of IP (5.659 eV) shows the easy removal of the electron cloud from the outermost orbital and the low value of EA (0.224 eV) shows the easy addition of the electron cloud to the electrophilic part. The CP shows the tendency of the molecule to form chemical bonds and undergo a chemical reaction. The negative value of CP (-2.941 eV) for Isoatisine shows the high reactivity of the molecule towards the chemical reactions. The high value of η (2.717 eV) shows that the Isoatisine molecule is hard and stiff. Thus, the FMO parameters clearly show the reactivity of the Isoatisine molecule.

The absorption band was also examined to justify the reactivity of the Isoatisine molecule. The UV-Vis spectra of Isoatisine were computed by energy optimization using time-dependent density functional theory (TD-DFT) and B3LYP/6311-G basis set. UV-Vis spectra of Isoatisine comprise one broad absorption band (Fig. 5(b)). Computed absorption excitation energies (E) and oscillator strength (f) corresponding to the transitions S0 →S1, S2, and S3 are mentioned in SD. 8. The maximum intensity peak for the Isoatisine molecule was reported at 210.42 nm wavelength with E 5.8922 eV which majorly imparts in the formation of the absorption band. The other major transitions were observed at 222.63 nm and 247.69 nm wavelength with E values of 5.5691 eV and 5.0056 eV respectively. These transitions are caused due to the existence of π→π* and n→π* bonds. Thus, the excitation of electrons shows the high reactivity of the probe molecule. The high excitation energies of the corresponding transitions, however, show the high binding ability of the ligand to bind to the active sites of the protein.

4.3 MD Simulation

Molecular dynamics is a computer-based simulation method that is used in studying the physical movements of the protein-ligand complex. The protein-ligand complex was put on to simulate in the thermodynamical ensemble for a duration of 50ns. Different parameters such that hydrogen bonds,

RMSD, RMSF, and Rg were computed for the Isoatisine + 7QNW complex, and the trajectories were illustrated in Fig. 6. The number of hydrogen bond interactions remained constant at 1 till 30 ns in the starting and rise to 2 for the last 50 ns of the time trajectory (Fig. 6(**a**)). This value is very near to the hydrogen bond interactions obtained in docking. The RMSD value of the complex was seen to fluctuate between 2 Å to 5 Å (Fig. 6(**b**)). This value shows the binding of ligand to the protein. The low is the RMSD, good will be the binding. However, the value of RMSF seems to fluctuate between 1 Å to 6 Å (Fig. 6(**c**)). The highly raised value of RMSF shows the flexibility of the molecular bonds. This flexibility can be considered an outcome of binding stability. Thus, the values of RMSD and RMSF are acceptable and reveal that the protein-ligand complex is highly stable and has a better stability. Moreover, the protein did not get affected throughout the simulation time due to the presence of ligand at the binding site. The Rg was computed to examine the compression of the protein-ligand complex. The value of Rg was seen to fluctuate between 38 Å to 41 Å (Fig. 6(**d**)). The high value of Rg shows the compactness of the complex. The results obtained from MD simulation show the high binding of Isoatisine with spike glycoprotein of COVID-19. Thus, the *in-silico* study justifies the potent ability of the Isoatisine molecule to inhibit the Omicron variant of COVID-19.

4.4 Molecular Mechanics Generalized Born and Surface Area (MMGBSA) calculations

To assess the binding energy of ligands to protein molecules, the MMGBSA technique is commonly employed. The binding free energy of each protein-ligand complex, as well as the impact of other non-bonded interaction energies, was estimated. With the ligand-free energy of binding energy was recorded (ΔG) -23.25 kcal/mol. Non-bonded interactions like $G_{bindCoulomb}$, $G_{bindCovalent}$, $G_{bindHbond}$, $G_{bindLipo}$, $G_{bindSolvGB}$, and $G_{bindvdW}$ govern G_{bind}. Across all types of interactions, the $G_{bindvdW}$, $G_{bindLipo}$, $G_{bindHbond}$, and $G_{bindSolvGB}$ energies contributed the most to the average binding energy. On the other side, the $G_{bindCoulomb}$ and $G_{bindCovalent}$ energies contributed the least to the final average binding energies. Furthermore, the $G_{bindHbond}$ interaction values of ligand-protein complexes demonstrated stable hydrogen bonds with amino acid residues. In all of the compounds, $G_{bindCoulomb}$ and $G_{bindCovalent}$ exhibited unfavorable energy contributions and so opposed binding. Pre-simulation (0 ns) and post-simulation (0 ns), a ligand in the binding pockets of protein has undergone a large angular change (45º) in the pose (Fig. 7, arrow). These conformational changes lead to better binding pocket acquisition and interaction with residues, which leads to enhanced stability and binding energy.

Thus, MM-GBSA calculations resulted, from MD simulation trajectories well justified with the binding energy obtained from docking results moreover, the last frame (100 ns) of MMGBSA displayed the positional change of the ligand as compared to the 0 ns trajectory signifying the better binding pose for best fitting in the binding cavity of the protein (Fig. 7).

5. Conclusion

The Omicron variant is the most swiftly mutating variant of COVID-19 and is widespread. The influence of this is observed as a severe catastrophe for humankind. The present study aims to find such herbal agents that will counter the Omicron variant. The *in-silico* study performed with the active phytochemicals of the medicinal herb 'Aconitum Heterophyllum' resulted from the inhibiting activity of Isoatisine against spike glycoprotein PDB ID: 7QNW of COVID-19. The molecular docking performed showed the high binding affinity of Isoatisine with the target macromolecule. This molecule also follows the ADMET properties showing the drug-like behavior. The reactivity had been checked for this molecule by DFT. The MEP surface and the displaced orbitals in the HOMO-LUMO surface show the displacement of the charge cloud from the pyrrolidine ring to the hydroxyl group and the availability of ICT. The π→π* and n→π* transitions obtained by electronic spectra also exist for the high wavelengths. These parameters combined show the high reactivity of the Isoatisine. The MD simulation done to further check the stability of the protein-ligand complex formed from docking shows favorable results. The low value was obtained for the RMSD and the high value for RMSF shows that the ligand is finely attached to the binding site of the target macromolecule and simulates the time trajectory of 50 ns without any hindrance. The values of Rg were also obtained highly raised showing the compactness and the high stability of the protein-ligand complex. Therefore, this study introduces Isoatisine as an emerging inhibitor against the Omicron variant of Coronavirus. The results obtained in this study reveal the better potentiality of the selected molecule and thus, can be used for experimental validations and clinical trials in the future.

Declarations

Funding

The authors declare that this research received no specific grant from any funding agency.

Conflict of interest:

The work: "Inhibiting Property of Phytoconstituents of 'Aconitum Heterophyllum' Against Omicron Variant of SARS-CoV-2: Molecular Docking, Molecular Dynamic and MM-GBSA approach" by Shradha Lakhera, Kamal Devlal, Arabinda Ghosh, and myself is original research work done by the authors. The authors declare that they have no known competing financial interests or personal relationships that could have appeared to influence the work reported in this paper.

Availability of data and material

Phytochemical structure: https://cb.imsc.res.in/imppat/home

Extension conversion: http://openbabel.org/wiki/Main_Page

Optimization: https://gaussian.com/

Data analysis: https://gaussian.com/gaussview6/

Graph plotting: https://www.originlab.com/

Protein structure: https://www.rcsb.org/

Molecular docking: https://vina.scripps.edu/

Docking analysis: https://discover.3ds.com/discovery-studio-visualizer-download

MD Simulation: https://www.gromacs.org/

Corresponding author

Correspondence to Dr. Meenakshi Rana

Author's contribution

Authors: Shradha Lakhera, Kamal Devlal, Meenakshi Rana, Ismail Celik

Shradha Lakhera: Data curation, Writing-Original draft preparation, Visualization, Investigation, Software, Validation.

Kamal Devlal: Conceptualization, Writing- Reviewing and Editing

Meenakshi Rana: Conceptualization, Methodology, Writing-Reviewing and Editing, Supervision

Arabinda Ghosh: Software handling, Reviewing and Editing

Declaration of competing interest

The authors declare that they have no known competing financial interests or personal relationships that could have appeared to influence the work reported in this paper.

References

1. Hirotsu Y, Omata M (2021) SARS-CoV-2 B.1.1.7 lineage rapidly spreads and replaces R.1 lineage in Japan: Serial and stationary observation in a community. MEEGID 95:105088, https://doi.org/10.1016/j.meegid.2021.105088
2. Eguia RT, Crawford KHD, Ayers TS, Millevolte LK, Greninger AL, Englund JA, Boeckh MJ, Bloom JD (2021) A human coronavirus evolves antigenically to escape antibody immunity. PLoS Pathog. 17:1009453. https://doi.org/10.1371/journal.ppat.1009453
3. Update on Omicron (2021) WORLD HEALTH ORGANIZATION https://www.who.int/news/item/28-11-2021-update-on-omicron
4. Wei C, Shan KJ, Wang W, Zhang S, Huan Q, Qian W (2021) Evidence for a mouse origin of the SARS-CoV-2 Omicron variant. J Genet Genomics 48(12):1111-1121.

https://doi.org/10.1016/j.jgg.2021.12.003

5. Metzger CMJA, Lienhard R, Smith HMBS, Roloff T, Wegner F, Sieber J, Bel M, Greub G, Egli A (2021) PCR performance in the SARS-CoV-2 Omicron variant of concern? Swiss Med Wkly.151:w30120. https://doi.org/10.4414/smw.2021.w30120

6. Tracking SARS-CoV-2 variants, World health organization (2021). https://www.who.int/en/activities/tracking-SARS-CoV-2-variants/

7. Gao Y, Cai C, Grifoni A, Müller TR, Niessl J, Olofsson A, Humbert M, Hansson L, Österborg A, Bergman P, Chen P, Olsson A, Sandberg JK, Weiskopf D, Price DA, Ljunggren HG, Karlsson AC, Sette A, Aleman S, Buggert M (2022) Ancestral SARS-CoV-2-specific T cells cross-recognize the Omicron variant. Nat. Med. https://doi.org/10.1038/s41591-022-01700-x

8. Kazybay B, Ahmad A, Mu C, Mengdesh D, Xie Y (2022) Omicron N501Y mutation among SARS-CoV-2 lineages: Insilico analysis of potent binding to tyrosine kinase and hypothetical repurposed medicine. 45:102242. https://doi.org/10.1016/j.tmaid.2021.102242

9. Dejnirattisai, W., Huo, J., Zhou, D., et al. (2022) SARS-CoV-2 Omicron-B.1.1.529 leads to widespread escape from neutralizing antibody responses, Cell (2022), doi: https://doi.org/10.1016/j.cell.2021.12.046

10. Viana R. et al. (2022) Rapid epidemic expansion of the SARS-CoV-2 Omicron variant in southern Africa. Nature https://doi.org/10.1038/s41586-022-04411-y

11. Lakhera S, Devlal K, Ghosh A, Rana M (2021) In Silico Investigation of Phytoconstituents of Medicinal Herb Piper Longum Against SARS-CoV-2 by Molecular Docking and Molecular Dynamics Analysis 100199. https://doi.org/10.1016/j.rechem.2021.100199

12. Lakhera S, Devlal, K., Ghosh, A, Rana M (2022) Modelling the DFT structural and reactivity study of feverfew and evaluation of its potential antiviral activity against COVID-19 using molecular docking and MD simulations. Chem. Pap. https://doi.org/10.1007/s11696-022-02067-6

13. Chowdhury P (2021) In silico investigation of phytoconstituents from Indian medicinal herb 'Tinospora cordifolia (giloy)' against SARS-CoV-2 (COVID-19) by molecular dynamics approach, J. Biomol. Struct. Dyn. 39(17):6792-6809. https://doi.org/10.1080/07391102.2020.1803968

14. Sharbidre A, Dhage P, Duggal H, Meshram R (2021) In silico Investigation of Tridax procumbens PhytoConstituents Against SARS-CoV-2 Infection. 11(4):12120-12148 https://doi.org/10.33263/BRIAC114.1212012148

15. Chowdhury P, Pathak P (2020) Neuroprotective immunity by essential nutrient Choline for the prevention of SARS CoV2 infections: An in silico study by molecular dynamics approach. Chem. Phys. Lett. 761:138057. https://doi.org/10.1016/j.cplett.2020.138057

16. Sher H. et al. (2021) *Aconitum balfourii* Stapf. *Aconitum ferox* Wall. ex. Ser. *Aconitum heterophyllum* Wall. ex Royle *Aconitum laeve* Royle *Aconitum naviculare* (Brühl) Stapf. *Aconitum spicatum* Stapf. *Aconitum violaceum* Jacq. ex Stapf var. *violaceum* Ranunculaceae. In: Kunwar R.M., Sher H., Bussmann R.W. (eds) Ethnobotany of the Himalayas. Ethnobotany of Mountain Regions. Springer, Cham. https://doi.org/10.1007/978-3-030-57408-6_10

17. Malhotra N, Sharma S (2021) Aconitum heterophyllum, Himalayan Medicinal Plants, Academic Press. 5-25. https://doi.org/10.1016/B978-0-12-823151-7.00015-5

18. Negi CS (2007) Changing face of polyculture in the Darma and Johaar valleys, Pithoragarh, Kumaun Himalayas, Int. J. Sustain. Dev. 14(4):428-436. https://doi.org/10.1080/13504500709469743

19. Thakur SD (2019) Phytochemical constituents of some important medicinal plants from Dachigam National Park, Srinagar, Jammu and Kashmir, The Pharma Innovation Journal 2019; 8(2):68-71.

20. Tsering J, Tag H, Gogoi BJ, Veer V (2016) Traditional Anti-poison Plants Used by the Monpa Tribe of Arunachal Pradesh. In: Vijay Veer, Gopalakrishnan R. (eds) Herbal Insecticides, Repellents and Biomedicines: Effectiveness and Commercialization. Springer. https://doi.org/10.1007/978-81-322-2704-5_10

21. Singh V, Kumar K, Purohit D, et al. (2021) Exploration of therapeutic applicability and different signaling mechanism of various phytopharmacological agents for treatment of breast cancer, Biomed. Pharmacother. 139:111584. https://doi.org/10.1016/j.biopha.2021.111584

22. Ahmad H, Ahmad S, Shah SAA, Latif A, Ali M, Khan FA, Tahir MN, Shaheen F, Wadood A, Ahmad M (2017) Antioxidant and anticholinesterase potential of diterpenoid alkaloids from Aconitum heterophyllum. Bioorg. Med. Chem. Lett. 25(13):3368-3376. https://doi.org/10.1016/j.bmc.2017.04.022.

23. Obaidullah NM, Ahmad M, Wadood N, Lodhi MA, Shaheen F, Iqbal M Choudhary (2009) New diterpenoid alkaloids from Aconitum heterophyllum Wall: Selective butyrylcholinestrase inhibitors, J Enzyme Inhib Med Chem. 24(1):47-51. https://doi.org/10.1080/14756360801906202

24. Wani TA, Kaloo ZA, Dangroo NA (2021) Aconitum heterophyllum Wall. ex Royle: A critically endangered medicinal herb with rich potential for use in medicine, Journal of Integrative Medicine. https://doi.org/10.1016/j.joim.2021.12.004

25. Frisch MJ, Trucks GW, Schlegel HB, et al (2009) Gaussian 09, Revision B. 01, Gaussian Inc., Wallingford CT, 121:150-166.

26. Becke AD (1993) Density-functional thermochemistry. III. The role of exact exchange, J. Chem. Phys. 98:5648. https://doi.org/10.1063/1.464913

27. Becke AD (1997) Density-functional thermochemistry. V. Systematic optimization of exchange-correlation functionals, J. Chem. Phys. 107:8554−8560. https://doi.org/10.1063/1.475007

28. Koopmans T (1933) Ordering of wave functions and eigenenergies to the individual electrons of an atom. Physica 1:104−113. https://doi.org/10.1016/S0031-8914(34)90011-2

29. Yadav P, Rana M, Chowdhury P (20210 DFT and MD simulation investigation of favipiravir as an emerging antiviral option against viral protease (3CLpro) of SARS-CoV-2, J. Mol. Struct. 1246:131253. https://doi.org/10.1016/j.molstruc.2021.131253

30. Dennington R, Keith T, Millam J (2007) GaussView, Version 4.1.2, Semichem, Inc., Shawnee Mission, KS.

31. Bowers KJ, Chow E, Xu H, Dror RO, Eastwood MP, Gregersen BA, Klepeis JL, Kolossvary I, Moraes MA, Sacerdoti FD, Salmon JK, Shan Y, Shaw DE (2006) "Scalable Algorithms for Molecular Dynamics

Simulations on Commodity Clusters, *Proceedings of the ACM/IEEE Conference on Supercomputing (SC06), Tampa, Florida,* 11-17.

32. Origin (Pro), Version Number (e.g. "Version 2021b"). OriginLab Corporation, Northampton, MA, USA.

33. Piao L, Chen Z, Li Q, Liu R, Song W, Kong R, Chang S (2019) Molecular dynamics simulations of wild type and mutants of SAPAP in complexed with Shank. 20(1):p.224.
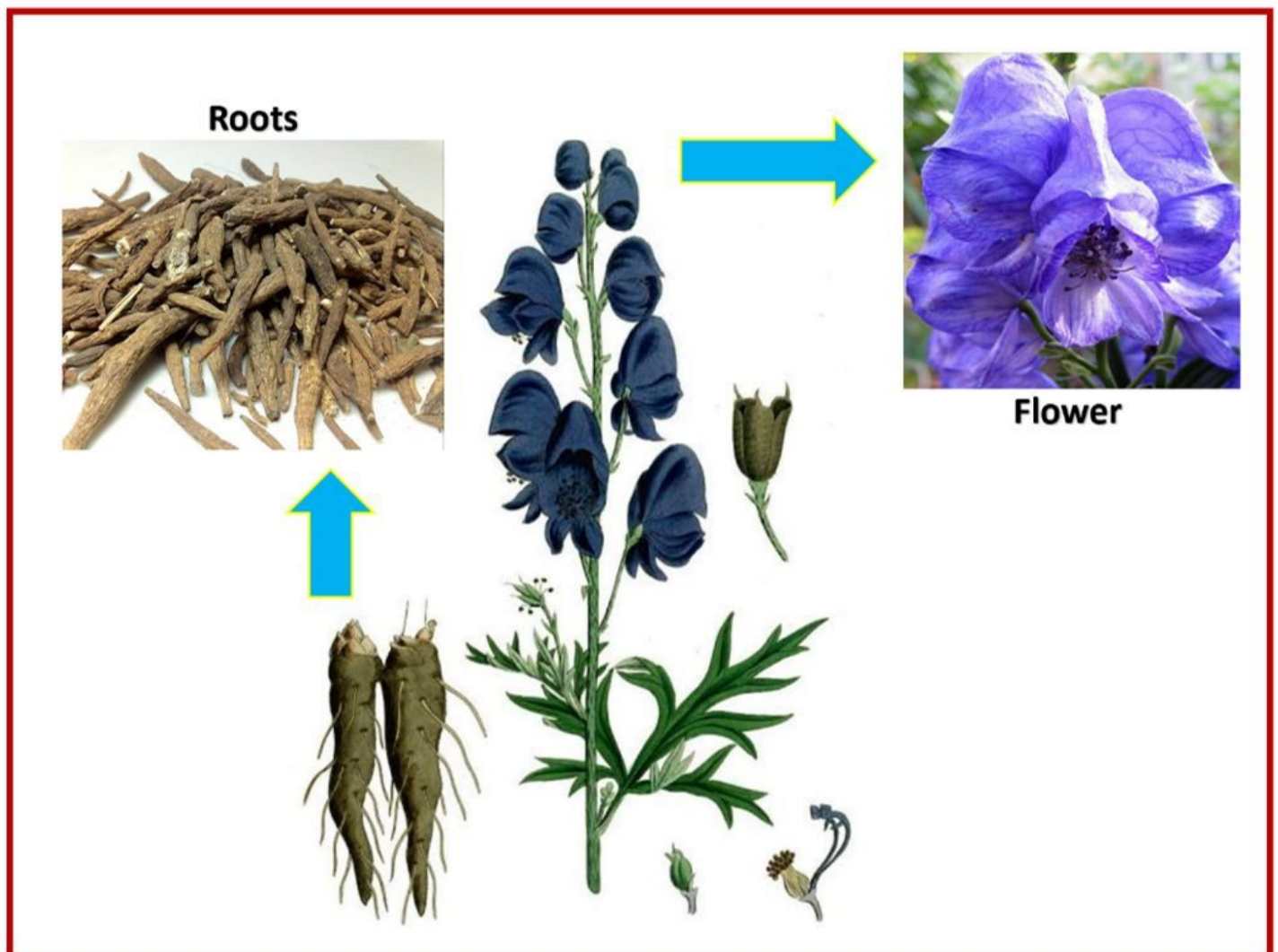
Figures

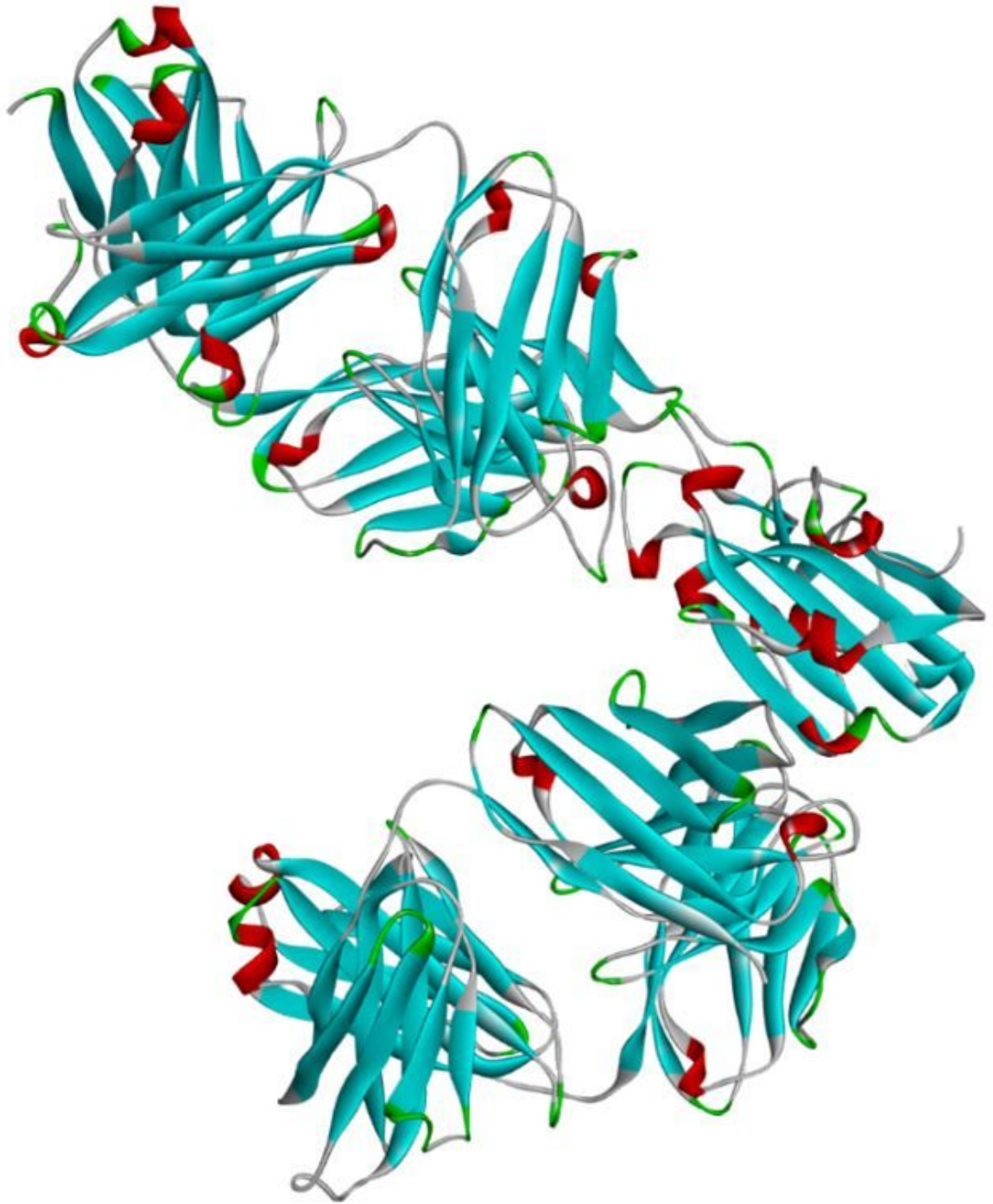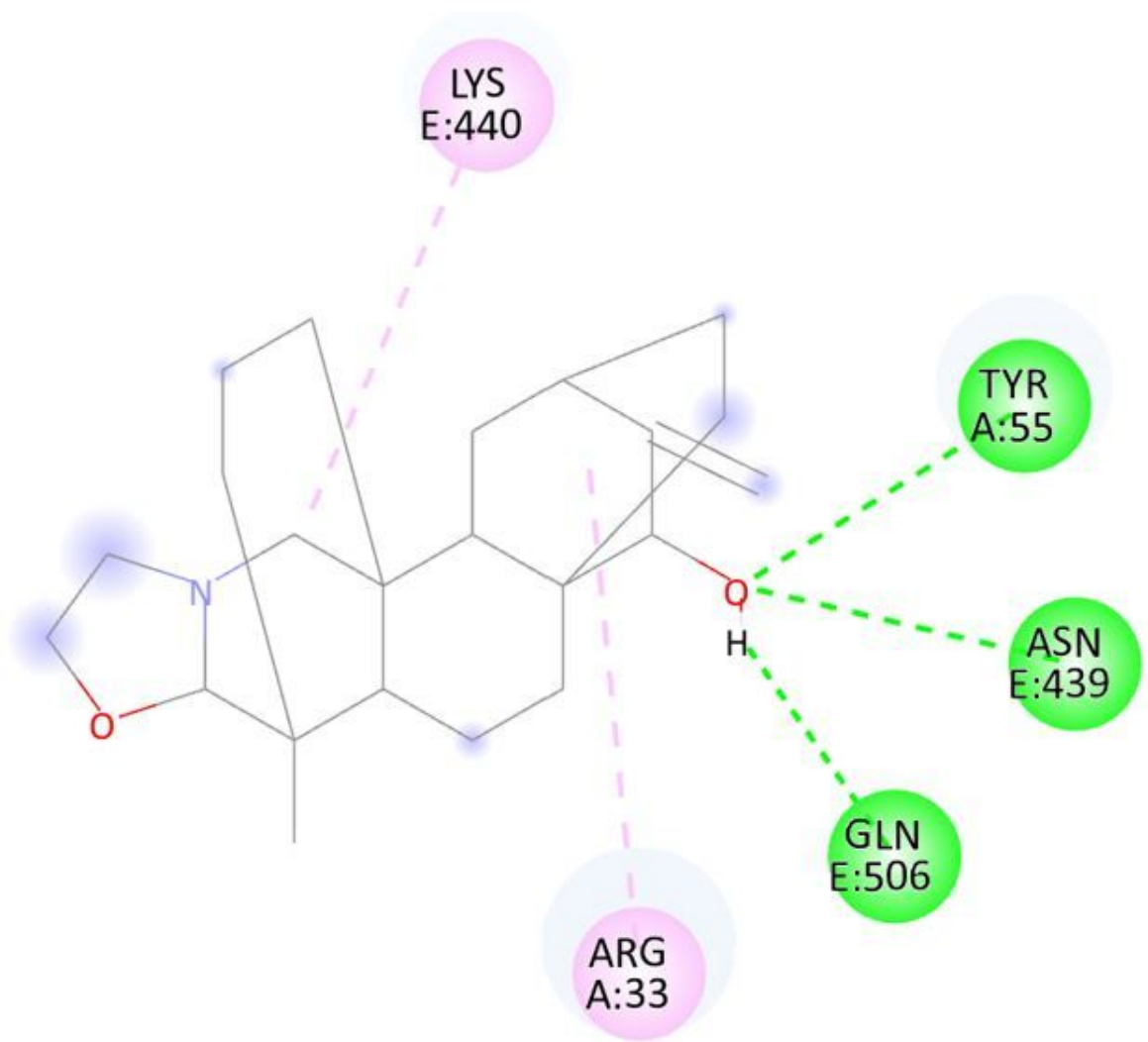

Figure 1

Morphology of the Aconitum Heterophyllum plant showing flower and roots.

Figure 2

Protein structure of omicron variant of SARS-CoV-2 with spike glycoprotein in complex with Beta-55 and EY6A (PDB ID: 7QNW).

Figure 3

2D view of conventional hydrogen bond and alkyl interactions associated to protein-ligand complex.
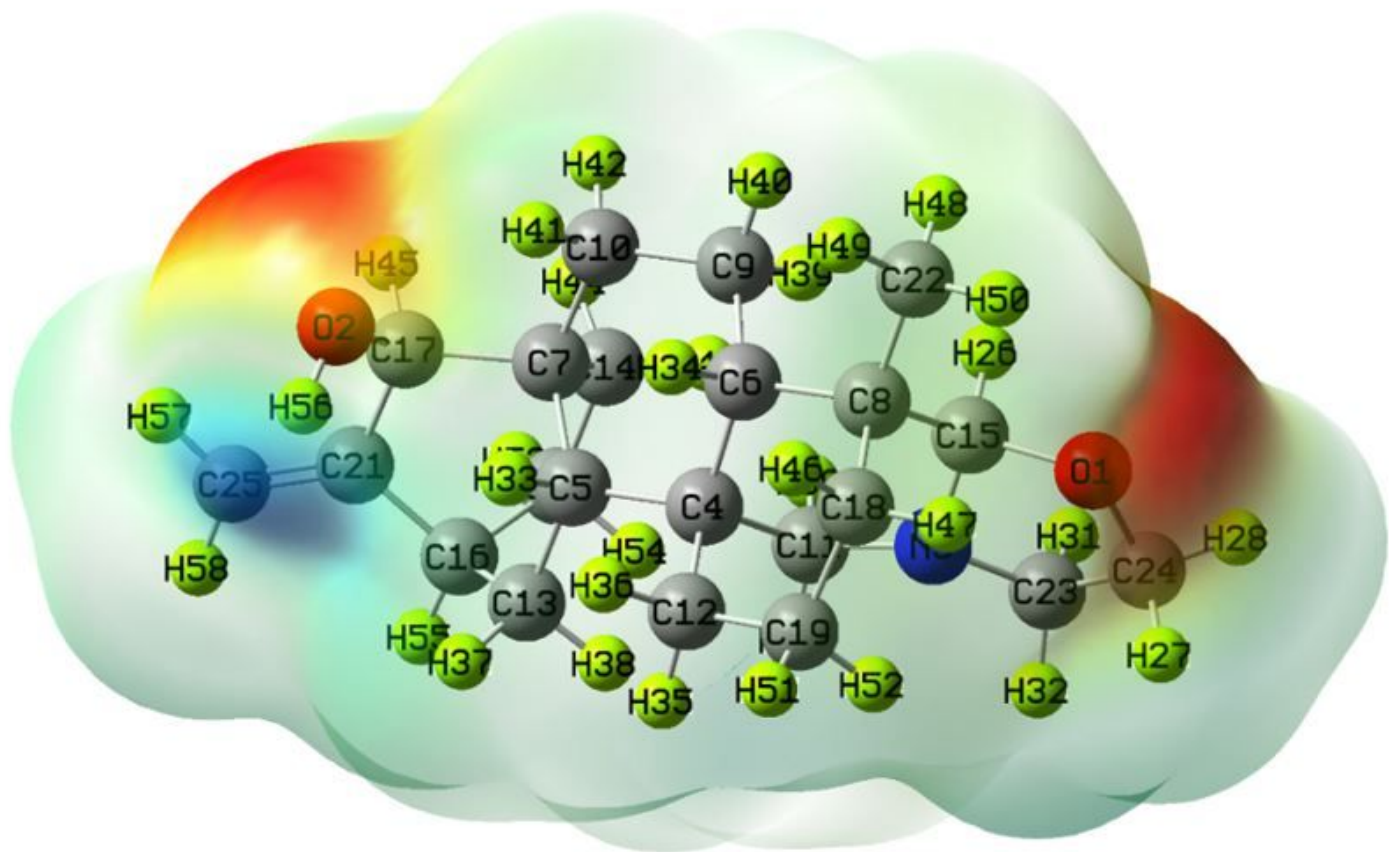
Figure 4

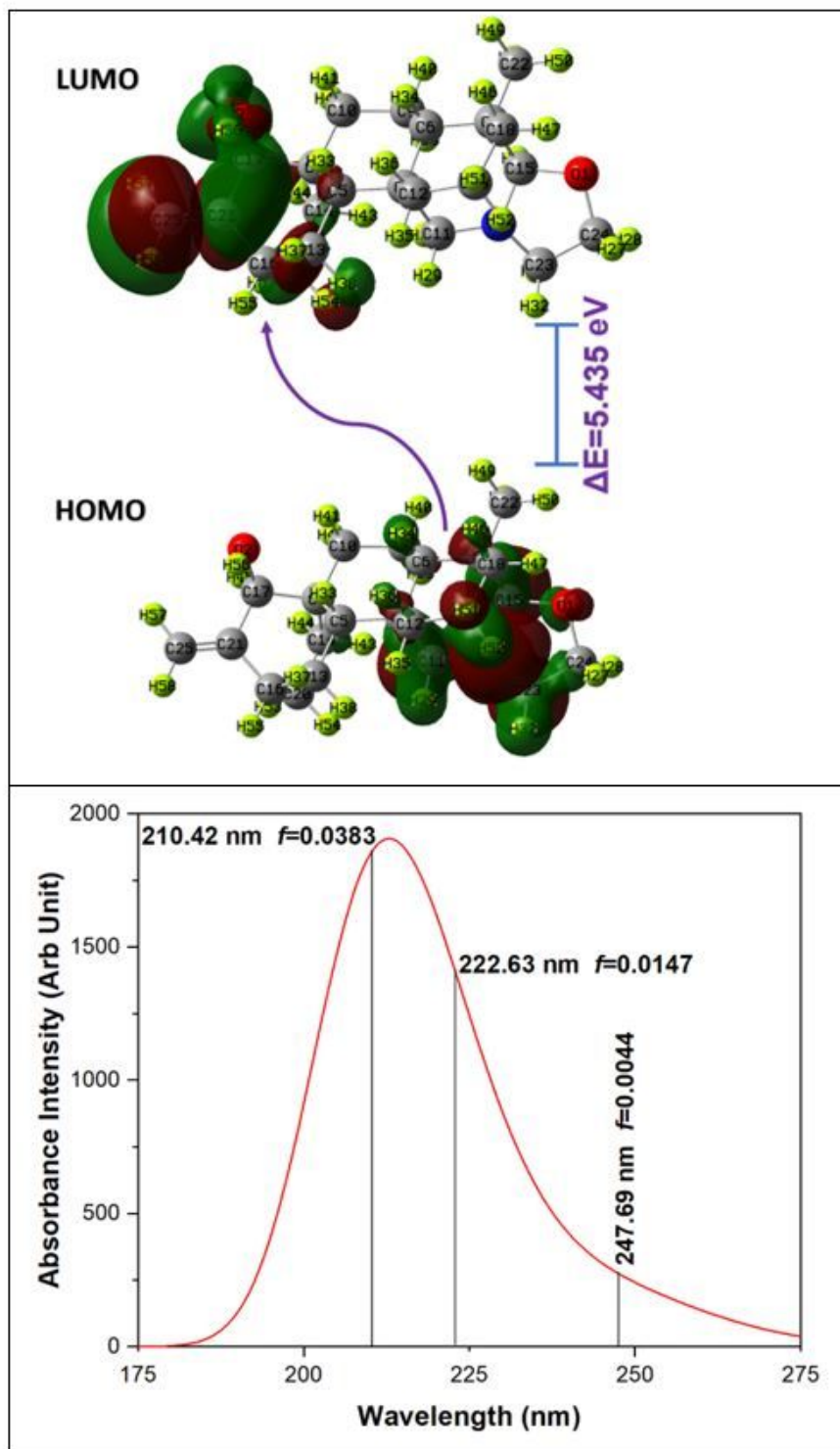Molecular electrostatic potential map of the Isoatisine molecule.

Figure 5

(a). HOMO-LUMO map of the Isoatisine molecule. The shifting of molecular surfaces from pyrrolidine ring to hydroxyl group indicates the ICT, (b) UV-Vis spectra of Isoatisine molecule.
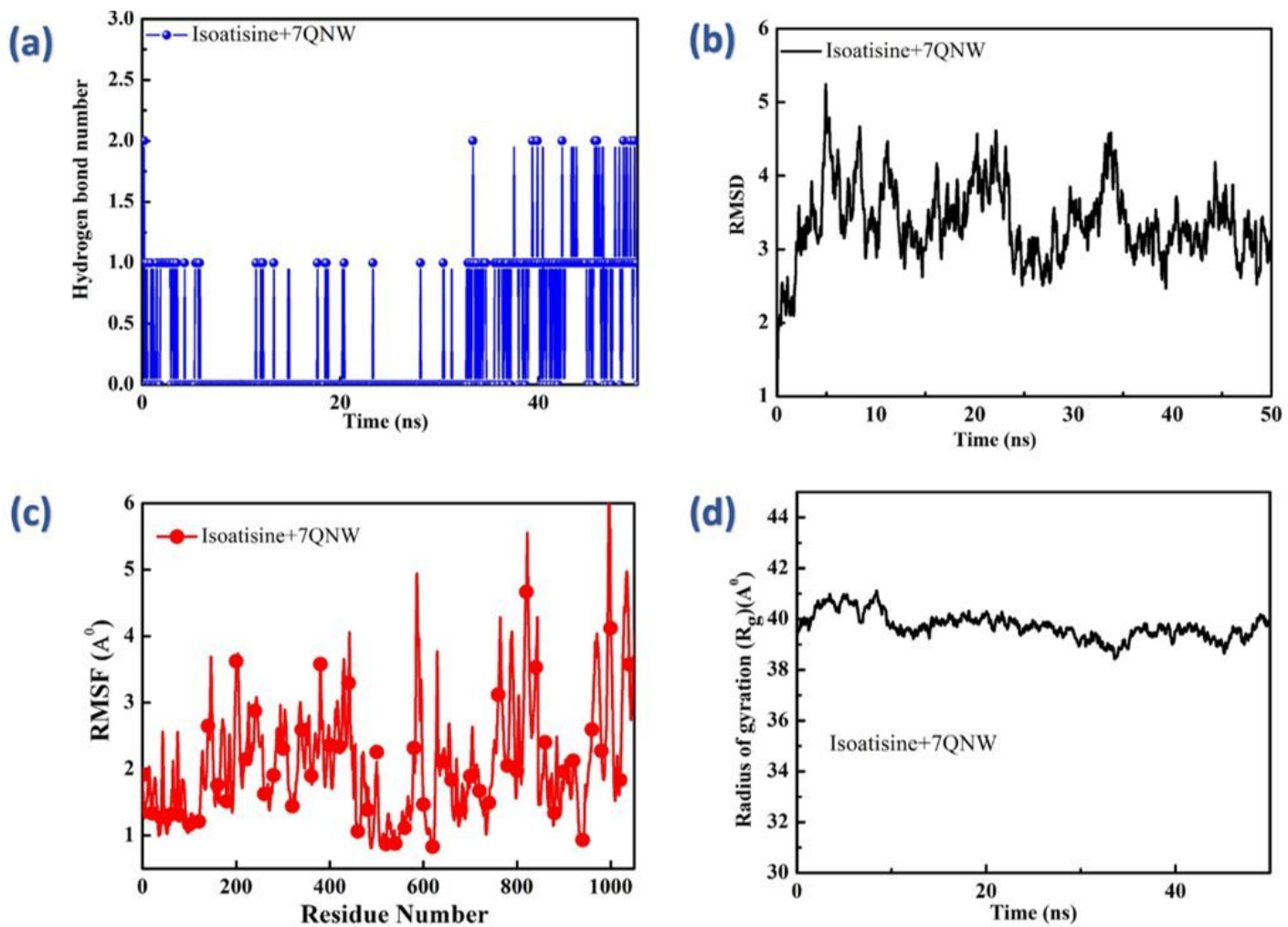
Figure 6

Trajectory analysis of molecular dynamics simulation of spike glycoprotein with Isoatisine **(a)** hydrogen bonds numbers, **(b)** RMSD of Isoatisine+7QNW, **(c)** RMSF of Isoatisine+7QNW **(d)** Rg values during the period of 50 ns simulation.
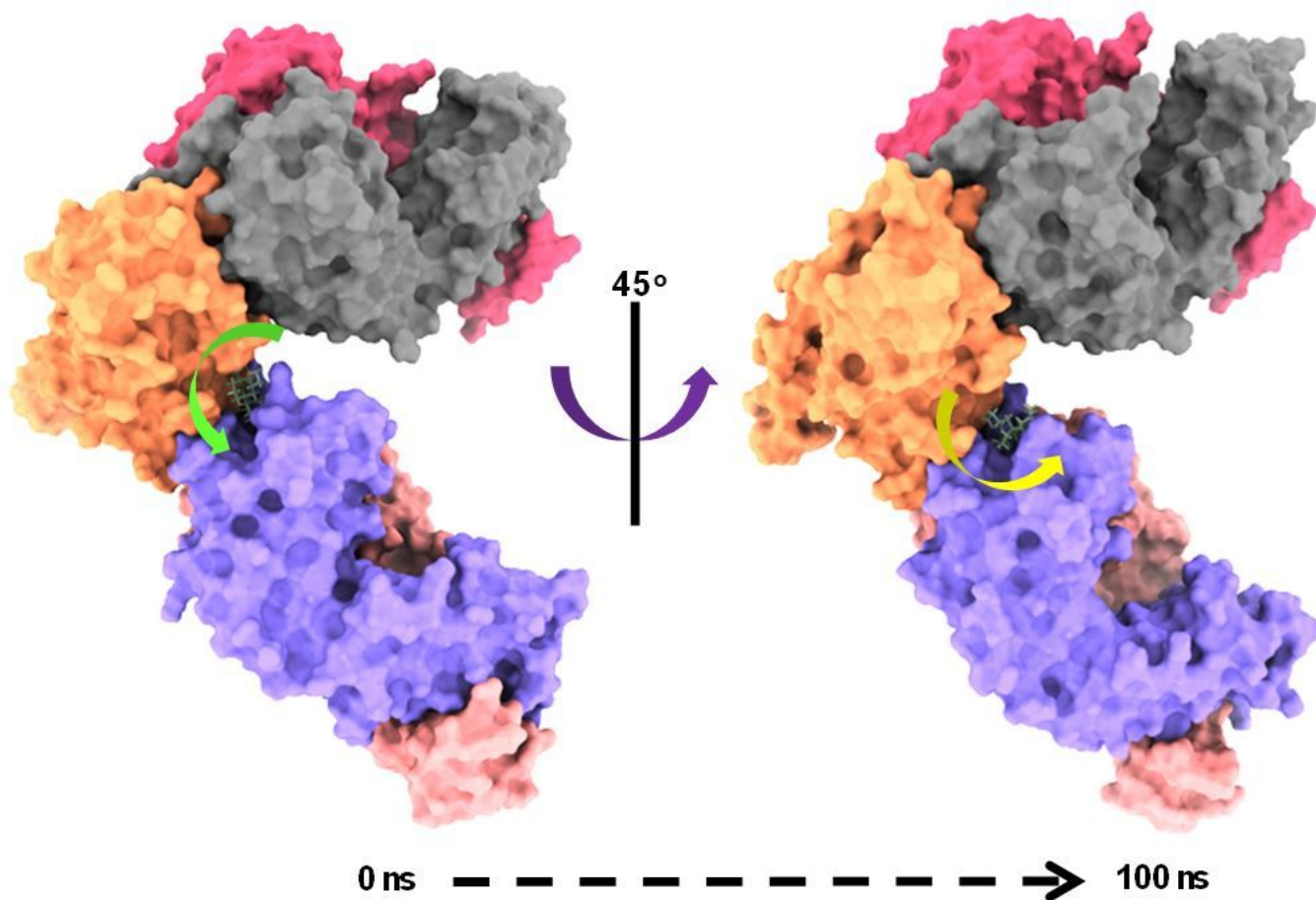
Figure 7

Location of ligand in binding pocket at 0ns and 100ns showing the angular change of 45º.

Supplementary Files

This is a list of supplementary files associated with this preprint. Click to download.

- GraphicalAbstract.pdf
- ResearchHighlight.docx
- Supportingdocument.docx